Spin transport in different oxide phases of copper

Rongxin Sha [iD],[1,2] Qinxi Liu [iD],[3] Mengyi Wang,[1,2] Min Liu [iD],[4] Yibo Peng,[4] Ziyang Zhang,[1,2] Ailiang Zou,[1,2] Yuekui Xu,[1,2] Xue Jiang [iD],[3,*] and Zhiyong Qiu [iD][1,2,†]

[1]*Key Laboratory of Materials Modification by Laser, Ion, and Electron Beams (Ministry of Education), School of Materials Science and Engineering, Dalian University of Technology, Dalian, 116024 Liaoning, China*
[2]*Key Laboratory of Energy Materials and Devices (Liaoning Province), School of Materials Science and Engineering, Dalian University of Technology, Dalian, 116024 Liaoning, China*
[3]*School of Physics, Dalian University of Technology, Dalian, 116024 Liaoning, China*
[4]*School of Mechanical Engineering, Dalian Jiaotong University, Dalian, 116024 Liaoning, China*

In this study, spin transport was directly compared in two types of copper oxides: The first is antiferromagnetic CuO, in which Cu^{2+} has one unpaired spin in the $3d$ orbital; the second is diamagnetic Cu_2O with a Cu^+ ion having a fully filled $3d$ orbital. The results indicate that CuO exhibits good spin conductivity, whereas Cu_2O is a spin insulator. This indicates that possessing unpaired spins may be an important characteristic of good spin conductors and that copper oxides may have the potential to be spin manipulators.

I. INTRODUCTION

Spin can be transported via an insulator even in the absence of free electron motion, implying that it is not affected by the Joule heating problem [1]. Since Kajiwara *et al.* demonstrated spin transport in insulating yttrium iron garnet (YIG) [2], electrical spin in insulators, rather than electrical charge, has been considered to serve as the carrier of information and energy in spin-based devices [3]. It has been observed that spin can be transported in various insulators [4–8], some of which may even enhance its efficiency [9–11]. The study of spin transport in insulators is important for developing insulating spin-based devices and is a central topic in spintronics [4,12,13]. Therefore, one of the most important challenges in spintronics is to understand the mechanisms and dominant characteristics of spin transport in insulating systems.

Spin transport has been actively investigated and discussed in the context of various insulating systems [4–17]. For nonmagnetic insulators, spin transport follows the tunneling mechanism by which most nonmagnetic insulators are spin insulators [15]. For magnetic insulators, the magnetic excitations can act as spin carriers; thus, many magnetic insulators exhibit good spin conductivities [3,18]. Furthermore, spin transport has been found to be sensitive to specific properties of magnetic materials. Spin susceptibility, for example, was found to be a governing factor for spin transport efficiency in an antiferromagnetic insulator [8,9]. The Néel vector is another explicit factor concerning spin transport in an antiferromagnetic insulator that has a definite uniaxial Néel vector and strong anisotropy energy [19]. However, the relationship between spin transport and intrinsic characteristics of the ambient material, such as phase, structure, defects, and even electronic configuration of the ions, is still rarely investigated.

In the present study, we focus on the influence of electronic configurations of ions on the spin transport efficiency in materials. Two types of copper oxides were selected in this study; although both of them are composed of copper and oxygen, the copper ions have different electronic configurations [20]. In CuO, the Cu^{2+} ion has one unpaired spin in the $3d$ orbital [Fig. 1(a)] [20], whereas in Cu_2O, the Cu^+ ion has a fully filled $3d$ orbital [Fig. 1(b)] [20]. It is well known that electronic configuration cannot be separated from the other materials characteristics, such as magnetic property and crystal structure. Thus, CuO and Cu_2O demonstrate different characteristics, where monoclinic CuO [21,22] is antiferromagnetic [23] while cubic Cu_2O [21] is diamagnetic [24]. By comparing the spin transport in these two oxides, it is possible to obtain information about the influence of metallic ions having different electronic configurations on spin transport.

A trilayer spin pumping structure [25] was used to study spin transport, wherein the copper oxide layer was sandwiched between a YIG layer and a heavy-metal (Pt) layer [Fig. 2(a)]. Within this structure, the YIG layer acted as a spin generator while the Pt layer acted as a spin detector [8,26]. Our results show that spin currents can be conducted through a 5 nm thick CuO film [Fig. 1(c)], which indicates that CuO is a good spin conductor. Contrarily, the spin currents were completely blocked by a 5 nm thick Cu_2O film [Fig. 1(d)], indicating that Cu_2O is a spin insulator. The different spin conducting properties between CuO and Cu_2O can thus be attributed to the electronic configurations of their copper ions, which can also be related to their magnetic properties and crystal structures.

II. EXPERIMENT

YIG/CuO/Pt and YIG/Cu_2O/Pt trilayer devices were developed as the target samples [Figs. 1(c) and 1(d)], and a fundamental YIG/Pt bilayer device was prepared as the control sample. Single-crystal YIG was grown on a $Gd_3Ga_5O_{12}$

*Corresponding author: jiangx@dlut.edu.cn
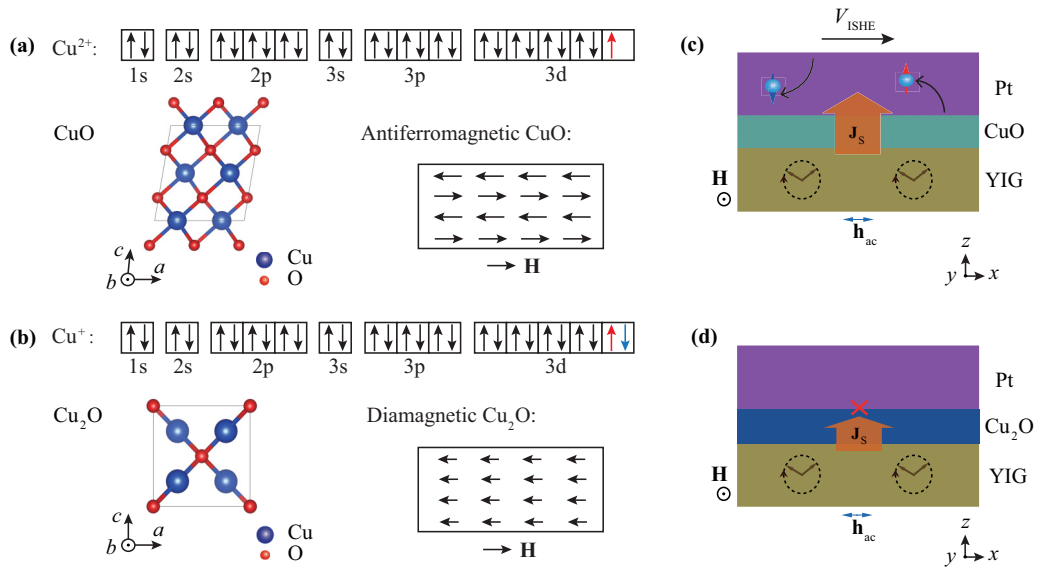†Corresponding author: qiuzy@dlut.edu.cn

FIG. 1. (a) The electronic structure, crystal structure, and magnetic property of CuO. (b) The electronic structure, crystal structure, and magnetic property of Cu_2O. (c) The concept of the spin transport in the YIG/CuO/Pt trilayer device. $\mathbf{J}_s$ denotes spin currents injected from the YIG layer into the Pt layer through the CuO layer by spin pumping, which is detected as a voltage signal V_{ISHE} via the inverse spin Hall effect in the Pt layer. (d) The concept of the spin transport in the YIG/Cu_2O/Pt trilayer device.

substrate by a liquid-phase epitaxy method. The YIG substrates of all the samples were cut from the same wafer to minimize differences among the samples. Copper oxide films of 5 nm thickness were deposited on the YIG layer from a metallic copper target in a mixture of Ar and O_2 gases using

FIG. 2. (a) The schematic of sample and experimental setup of spin pumping effect. (b) The x-ray diffraction patterns of the CuO and Cu_2O films displayed on a linear scale. (c) Magnetic field (H) dependence of microwave absorption spectrum for the YIG/Pt, YIG/CuO (5 nm)/Pt, and YIG/Cu_2O (5 nm)/Pt devices at $T = 300$ K. (d) Magnetic field (H) dependence of electric voltage (V) detected in the YIG/Pt, YIG/CuO (5 nm)/Pt, and YIG/Cu_2O (5 nm)/Pt devices at $T = 300$ K.

a reactive magnetron sputtering system at room temperature. The total pressure of the mixed gas was set to 3 Pa, in which $p(O_2)/p(O_2 + $ Ar$)$ was 33%. A post-annealing process was employed to modify the chemical valences of the copper ions, by which CuO was obtained at $500\,^\circ$C after 1 h whereas Cu_2O was generated at $700\,^\circ$C after 1 h. Both these films were annealed in the Ar and O_2 gas mixture under 3 Pa for CuO and 5×10^{-5} Pa for Cu_2O; a 10 nm thick Pt film was then deposited on both samples in the same sputtering chamber.

CuO and Cu_2O were then identified using x-ray diffraction measurements [Fig. 2(b)]. The monoclinic CuO film shows a single sharp (11-1) pattern, and the cubic Cu_2O film shows both the (111) and (200) patterns, suggesting that the CuO film exhibits a preferred orientation whereas the Cu_2O film exhibits random orientation. As the full width at half maximum of CuO and Cu_2O films are almost the same, their nominal grain sizes should be similar. Therefore, the discrepancy of peak intensity between the films can mainly be attributed to the different orientations.

Spin transport in different devices were studied using a spin pumping setup [Fig. 2(a)] [8,26]. The trilayer device was placed at the end of a short-end coplanar waveguide, using which microwaves were applied at a frequency of 6 GHz [Fig. 2(a)]. The microwaves and an external magnetic field H thus excited ferromagnetic resonance (FMR) in the YIG layer. Then, spin currents were generated and injected into the copper oxide layers by the spin pumping effect [25]. The spin currents that are conducted through the middle oxide layer will be detected as voltage signals via the inverse spin Hall effect (ISHE) in the Pt layer [27].
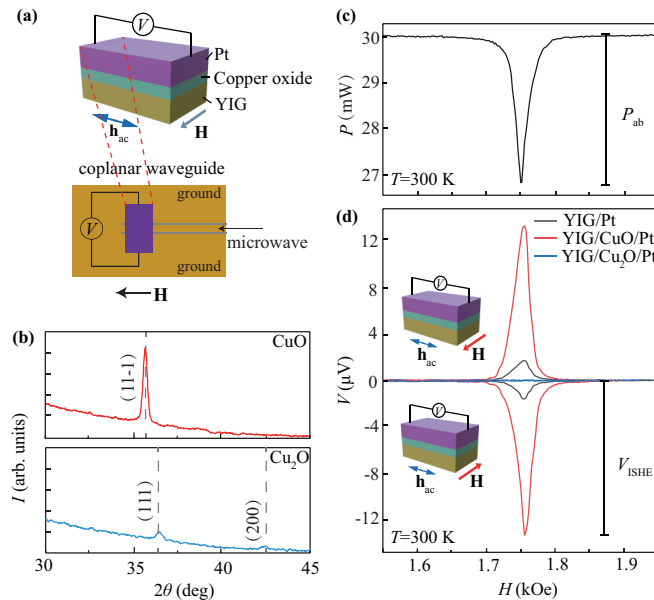
III. RESULTS AND DISCUSSION

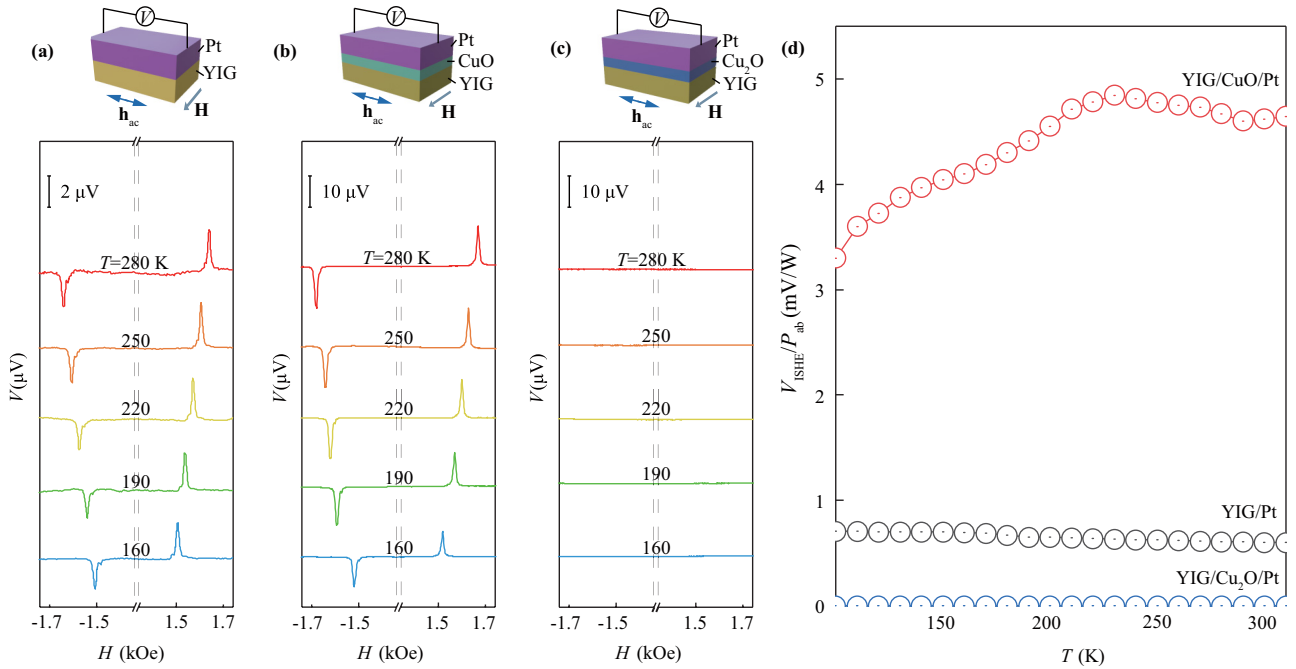A typical microwave absorption spectrum is shown in Fig. 2(c), where the microwave absorption peak can be

FIG. 3. (a)–(c) Magnetic field (H) dependence of electric voltage (V) detected in the YIG/Pt, YIG/CuO (5 nm)/Pt, and YIG/Cu$_2$O (5 nm)/Pt devices at various temperatures with evenly spaced offset in vertical axis. (d) Temperature dependence of V_{ISHE}/P_{ab} for the YIG/Pt, YIG/CuO (5 nm)/Pt, and YIG/Cu$_2$O (5 nm)/Pt devices.

observed at $H_{FMR} = 1.76$ kOe when $T = 300$ K; here, H_{FMR} corresponds to the FMR of the YIG layer. The microwave absorption power P_{ab} was defined as the height of the microwave absorption peak [Fig. 2(c)]. For all samples, the positions and heights of the microwave absorption peaks are almost similar because the YIG substrates were cut from the same wafer. Therefore, the YIG substrates can be considered as stable spin generators in all samples. With regard to the magnetic field (H) dependence of electric voltage (V), the voltage peaks were obtained at the same H_{FMR} [Fig. 2(d)]. Here, the electric voltage V was set to zero where the FMR was not excited (see Supplemental Material Fig. 1 [28]); this is a commonly practiced data processing method for spin pumping [8,9]. The signs of the voltage peaks were reversed when the external magnetic field was reversed, suggesting that the voltage peaks are the induced ISHE signals in the Pt layer by spin currents pumped from the YIG layer. Herein, we define the height of the voltage peak as the magnitude of the spin pumping signal V_{ISHE} [Fig. 2(d)].

CuO, with one unpaired spin in Cu^{2+}, exhibits spin conductive behavior. The V_{ISHE} of the YIG/CuO/Pt trilayer device is approximately 12 μV at $T = 300$ K [Fig. 2(d)]. This indicates that spin currents are conducted through the 5 nm thick CuO film. Furthermore, the V_{ISHE} of the YIG/CuO/Pt trilayer device is almost six times the magnitude of that of the YIG/Pt bilayer device, thereby implying that the CuO middle layer enhanced the spin transport efficiency at the YIG/Pt interface. Spin transport enhancement similar to the CuO middle layer in this study was also reported for a NiO middle layer in a previous work [9]. Currently, this enhancement phenomenon cannot be explained using existing theories and needs further investigation by researchers. In contrast to CuO, Cu$_2$O without the unpaired spin in Cu$^+$ acts as a spin insulator because

no voltage peaks are observed in the YIG/Cu$_2$O/Pt trilayer device. It is possible that the magnitudes of any existing voltage peaks might be less than the 30 nV noise level of our experiment, indicating that such spin currents were blocked by the 5 nm thick Cu$_2$O layer.

The magnetic field H dependence of the electric voltage V was measured at various temperatures for the YIG/Pt, YIG/CuO/Pt, and YIG/Cu$_2$O/Pt devices [Figs. 3(a), 3(b), and 3(c), respectively]. Voltage peaks can be observed in both the YIG/Pt and YIG/CuO/Pt devices at all temperatures. The positions of these peaks shift toward the direction of low magnetic field with decreasing temperatures, which corresponds to the dependence of the temperature dependence on the FMR condition in the YIG layer [8,29]. Furthermore, the signs of these voltage peaks are reversed by reversing the applied magnetic field, thereby confirming that the voltage peaks are related to the spin currents generated from the YIG layer via the spin pumping effect. On the contrary, no voltage peaks were observed in the YIG/Cu$_2$O/Pt trilayer device at any temperature.

The temperature dependences of spin pumping signals V_{ISHE} of the YIG/Pt, YIG/CuO/Pt, and YIG/Cu$_2$O/Pt devices are shown in Fig. 3(d). Here, V_{ISHE} is normalized by the microwave absorption power P_{ab} as V_{ISHE}/P_{ab}. In the YIG/Pt bilayer device, the V_{ISHE}/P_{ab} is almost constant over the entire range of temperatures, which is consistent with trends noted in other published reports [2,30]. However, by inserting a 5 nm thick CuO layer between the YIG and Pt layers, a clear peak of V_{ISHE}/P_{ab} was observed at $T = 230$ K, which is approximately equal to the Néel temperature of CuO. The observation that spin transport efficiency is maximized at the Néel temperature is consistent with that reported in previous studies [8,10]. Meanwhile, V_{ISHE} is suppressed on both sides of the
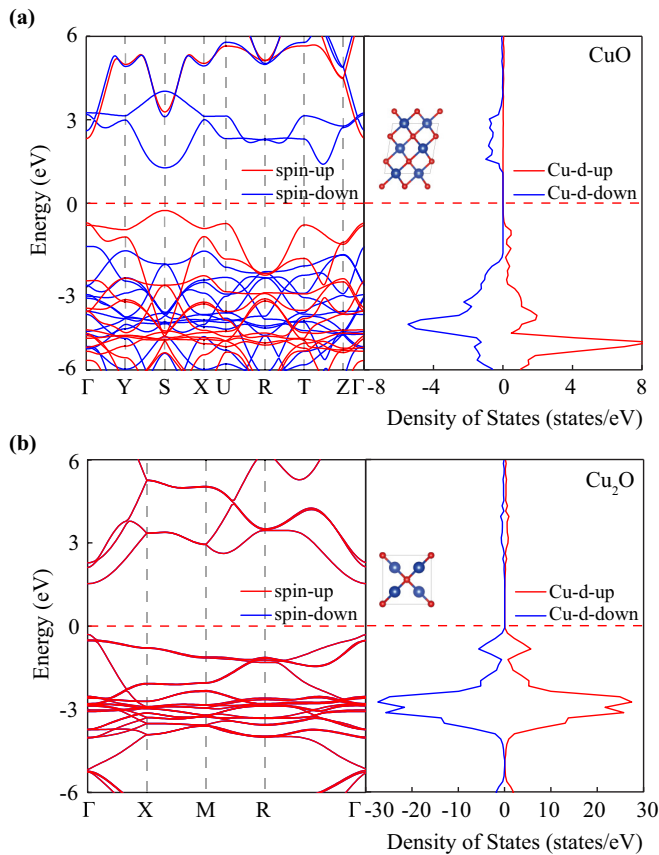
(a)

(b)

FIG. 4. (a) The band structure and density of states for CuO. (b) The band structure and density of states for Cu_2O. The red dashed lines indicate the Fermi level.

Néel temperature, which may be because the main carriers of spins are the thermally excited magnons in antiferromagnets [8]. Conversely, spin currents are blocked by the 5 nm thick Cu_2O layer at all temperatures.

CuO and Cu_2O exhibit different magnetic properties and structures owing to the electrical configurations of their ions. As seen from the calculated band structures using the HSE06 functional [31] in Fig. 4, both CuO and Cu_2O are typical electrical insulating materials with band gaps of 2.59 eV and 1.83 eV, respectively. In CuO, the spin-up and spin-down band

structures are different around the Fermi level. By comparing the energies of several typical types of magnetic ordering, we prove that the Cu atoms in CuO prefer the antiferromagnetic ordering. The antiferromagnetic ground state can be explained as a consequence of the unpaired spin in the $d_{x^2-y^2}$ orbital of the Cu^{2+} ion. On the contrary, Cu_2O exhibits diamagnetic properties. The spin-up and spin-down band structures are almost identical, and the spin band gap of Cu_2O is equivalent to its electron band gap. As a result, the spins are decoupled from each other in Cu_2O.

We attribute the different spin transport properties of CuO and Cu_2O to their different electronic configurations of copper ions. In CuO, the unpaired spins couple with each other, and the collective excitation acts as the carrier for the transported spins. Spin transport in such antiferromagnetic systems has been reported in several existing studies [4,8]. In Cu_2O, the spins are decoupled from each other, which prevents coherent excitation. As a result, the diamagnetic Cu_2O exhibits spin insulativity. Our study experimentally shows that unpaired spins are an important prerequisite for a good spin conductor. The observation that spin transport is affected by the electronic configuration of the ions offers a unique approach to realizing a new type of spin-current switch for a spin current transistor or memory.

IV. SUMMARY

In summary, our study found that possessing unpaired spins may be an important characteristic of a spin conductor. We compared spin transport in two different oxide phases of copper and found that CuO was a good spin conductor whereas Cu_2O was a spin insulator, which confirmed that spin transport was sensitive to electronic configurations of the constituent ions. Our results show the physical mechanism of spin transport in insulators and provide an approach for the manipulation of spin-based devices.

ACKNOWLEDGEMENTS

[1] S. Maekawa, *Concept in Spin Electronics* (Oxford University Press, Oxford, 2006).

[2] Y. Kajiwara, K. Harii, S. Takahashi, J. Ohe, K. Uchida, M. Mizuguchi, H. Umezawa, H. Kawai, K. Ando, K. Takanashi, S. Maekawa, and E. Saitoh, Transmission of electrical signals by spin-wave interconversion in a magnetic insulator, Nature (London) **464**, 262 (2010).

[3] S. A. Wolf, D. D. Awschalom, R. A. Buhrman, J. M. Daughton, S. von Molnár, M. L. Roukes, A. Y. Chtchelkanova, and D. M. Treger, Spintronics: A spin-based electronics vision for the future, Science **294**, 1488 (2001).

[4] D. Z. Hou, Z. Y. Qiu, and E. Saitoh, Spin transport in antiferromagnetic insulators: progress and challenges, NPG Asia Mater. **11**, 35 (2019).

[5] D. Z. Hou, Z. Y. Qiu, J. Barker, K. J. Sato, K. Yamamoto, S. Vélez, J. M. Gomez-Perez, L. E. Hueso, F. Casanova, and E. Saitoh, Tunable Sign Change of Spin Hall Magnetoresistance in Pt/NiO/YIG Structures, Phys. Rev. Lett. **118**, 147202 (2017).

[6] T. Ikebuchi, T. Moriyama, H. Mizuno, K. Oda, and T. Ono, Spin Current Transmission in Polycrystalline NiO Films, Appl. Phys. Express **11**, 073003 (2018).

[7] Y. M. Hung, C. Hahn, H. C. Chang, M. Z. Wu, H. Ohldag, and A. D. Kent, Spin transport in antiferromagnetic NiO and magnetoresistance in $Y_3Fe_5O_{12}$/NiO/Pt structures, AIP Adv. **7**, 055903 (2017).

[8] Z. Y. Qiu, J. Li, D. Z. Hou, E. Arenholz, A. T. N'Diaye, A. Tan, K. Uchida, K. Sato, S. Okamoto, Y. Tserkovnyak, Z. Q. Qiu, and E. Saitoh, Spin-current probe for phase transition in an insulator, Nat. Commun. **7**, 12670 (2016).

[9] H. L. Wang, C. H. Du, P. C. Hammel, and F. Y. Yang, Antiferromagnonic Spin Transport from $Y_3Fe_5O_{12}$ into NiO, Phys. Rev. Lett. **113**, 097202 (2014).

[10] L. C. Jin, K. C. Jia, D. N. Zhang, B. Liu, H. Meng, X. L. Tang, Z. Y. Zhong, and H. W. Zhang, Effect of interfacial roughness spin scattering on the spin current transport in YIG/NiO/Pt heterostructures, ACS Appl. Mater. Interfaces **11**, 35458 (2019).

[11] L. Baldrati, C. Schneider, T. Niizeki, R. Ramos, J. Cramer, A. Ross, E. Saitoh, and M. Kläui, Spin transport in multilayer systems with fully epitaxial NiO thin films, Phys. Rev. B **98**, 014409 (2018).

[12] L. J. Cornelissen, J. Liu, R. A. Duine, J. Ben Youssef, and B. J. van Wees, Long-distance transport of magnon spin information in a magnetic insulator at room temperature, Nat. Phys. **11**, 1022 (2015).

[13] A. Rückriegel and R. A. Duine, Long-Range Phonon Spin Transport in Ferromagnet-Nonmagnetic Insulator Heterostructures, Phys. Rev. Lett. **124**, 117201 (2020).

[14] T. Moriyama, S. Takei, M. Nagata, Y. Yoshimura, N. Matsuzaki, T. Terashima, Y. Tserkovnyak, and T. Ono, Anti-damping spin transfer torque through epitaxial nickel oxide, Appl. Phys. Lett. **106**, 162406 (2015).

[15] C. Hahn, G. De Loubens, V. V. Naletov, J. Ben Youssef, O. Klein, and M. Viret, Conduction of spin currents through insulating antiferromagnetic oxides, Epl **108**, 57005 (2014).

[16] H. L. Wang, C. H. Du, P. C. Hammel, and F. Y. Yang, Spin transport in antiferromagnetic insulators mediated by magnetic correlations, Phys. Rev. B **91**, 220410(R) (2015).

[17] A. Prakash, J. Brangham, F. Y. Yang, and J. P. Heremans, Spin Seebeck effect through antiferromagnetic NiO, Phys. Rev. B **94**, 014427 (2016).

[18] K. M. D. Hals, Y. Tserkovnyak, and A. Brataas, Phenomenology of Current-Induced Dynamics in Antiferromagnets, Phys. Rev. Lett. **106**, 107206 (2011).

[19] Z. Y. Qiu, D. Z. Hou, J. Baker, K. Yamamoto, O. Gomonay, and E. Saitoh, Spin colossal magnetoresistance in an antiferromagnetic insulator, Nat. Mater. **17**, 577 (2018).

[20] J. Ghijsen, L. H. Tjeng, J. van Elp, H. Eskes, J. Westerink, G. A. Sawatzky, and M. T. Czyzyk, Electronic structure of Cu_2O and CuO, Phys. Rev. B **38**, 11322 (1988).

[21] W. Y. Ching, Y. N. Xu, and K. W. Wong, Ground-state and optical properties of Cu_2O and CuO crystals, Phys. Rev. B **40**, 7684 (1989).

[22] S. Åsbrink and L. J. Norrby, A refinement of the crystal structure of copper(II) oxide with a discussion of some exceptional e.s.d.'s, Acta Crystallogr., Sect. B: Struct. Crystallogr. Cryst. Chem. B **26**, 8 (1970).

[23] A. Zúñiga, L. Fonseca, J. A. Souza, C. Rivaldo-Gomez, C. D. Pomar, and D. Criado, Anomalous ferromagnetic behavior and size effects in CuO nanowires, J. Magn. Magn. Mater. **471**, 77 (2019).

[24] C. P. Chen, L. He, L. Lai, H. Zhang, J. Lu, L. Guo, and Y. D. Li, Magnetic properties of undoped Cu_2O fine powders with magnetic impurities and/or cation vacancies, J. Phys. Condens. Matter **21**, 145601 (2009).

[25] K. Ando, S. Takahashi, J. Ieda, Y. Kajiwara, H. Nakayama, T. Yoshino, K. Harii, Y. Fujikawa, M. Matsuo, S. Maekawa, and E. Saitoh, Inverse spin-Hall effect induced by spin pumping in metallic system, J. Appl. Phys. **109**, 103913 (2011).

[26] Z. Qiu, T. An, K. Uchida, D. Hou, Y. Shiomi, Y. Fujikawa, and E. Saitoh, Experimental investigation of spin Hall effect in indium tin oxide thin film, Appl. Phys. Lett. **103**, 182404 (2013).

[27] E. Saitoh, M. Ueda, H. Miyajima, and G. Tatara, Conversion of spin current into charge current at room temperature: Inverse spin-Hall effect, Appl. Phys. Lett. **88**, 182509 (2006).

[28] See Supplemental Material at http://link.aps.org/supplemental/10.1103/PhysRevB.103.024432 for the original data of spin pumping experiments.

[29] I. Laulicht, J. T. Suss, and J. Barak, The temperature dependence of the ferromagnetic and paramagnetic resonance spectra in thin yttrium-iron-garnet films, J. Appl. Phys. **70**, 2251 (1991).

[30] Y. M. Lu, Y. Choi, C. M. Ortega, X. M. Cheng, J. W. Cai, S. Y. Huang, L. Sun, and C. L. Chien, Pt magnetic polarization on $Y_3Fe_5O_{12}$ and magnetotransport characteristics, Phys. Rev. Lett. **110**, 147207 (2013).

[31] J. Paier, M. Marsman, K. Hummer, G. Kresse, I. C. Gerber, and J. G. Angyán, Screened hybrid density functionals applied to solids, J. Chem. Phys. **124**, 154709 (2006).